Phytoplankton niche generation by interspecific stoichiometric variation

L. Göthlich[1] and A. Oschlies[1]

Received 27 January 2011; revised 16 October 2011; accepted 19 March 2012; published 3 May 2012.

[1] For marine biogeochemical models used in simulations of climate change scenarios, the ability to account for adaptability of marine ecosystems to environmental change becomes a concern. The potential for adaptation is expected to be larger for a diverse ecosystem compared to a monoculture of a single type of (model) algae, such as typically included in biogeochemical models. Recent attempts to simulate phytoplankton diversity in global marine ecosystem models display remarkable qualitative agreement with observed patterns of species distributions. However, modeled species diversity tends to be systematically lower than observed and, in many regions, is smaller than the number of potentially limiting nutrients. According to resource competition theory, the maximum number of coexisting species at equilibrium equals the number of limiting resources. By simulating phytoplankton communities in a chemostat model and in a global circulation model, we show here that a systematic underestimate of phytoplankton diversity may result from the standard modeling assumption of identical stoichiometry for the different phytoplankton types. Implementing stoichiometric variation among the different marine algae types in the models allows species to generate different resource supply niches via their own ecological impact. This is shown to increase the level of phytoplankton coexistence both in a chemostat model and in a global self-assembling ecosystem model.

Citation: Göthlich, L., and A. Oschlies (2012), Phytoplankton niche generation by interspecific stoichiometric variation, *Global Biogeochem. Cycles*, *26*, GB2010, doi:10.1029/2011GB004042.

1. Introduction

[2] Owing to global warming, environmental conditions controlling upper ocean biological production are expected to change significantly during this century: Rising surface temperatures and enhanced fresh-water input are expected to result in shallower mixed layers, leading to reduced upper-ocean nutrient supply [*Sarmiento et al.*, 1998]. In the oligotrophic areas of the tropical and subtropical ocean, this may cause a decline in phytoplankton abundance and primary production [*Behrenfeld et al.*, 2006; *Boyce et al.*, 2010]. Additionally, oligotrophic areas are expanding, which further decreases global ocean productivity [*Gregg et al.*, 2005; *Polovina et al.*, 2008].

[3] Marine plankton ecosystems are thus experiencing considerable environmental changes. Responses include changes in species physiology, species distribution and community composition [*Hays et al.*, 2005; *Richardson and Schoeman*, 2004; *Hoegh-Guldberg and Bruno*, 2010]. Still, the adaptation potential of marine ecosystems to environmental changes is poorly known, making estimates about their future evolution problematic. This even holds for phytoplankton at the base of the marine food chain and being an important agent in the cycling of nutrients and carbon.

[4] Modeling adaptive responses of phytoplankton to climate change requires a sufficiently diverse model community to allow for an adequate representation of the potential for adaptation [*McCann*, 2000]. Approaches to model phytoplankton diversity have been developed recently [*Bruggeman and Kooijman*, 2007; *Follows et al.*, 2007; *Shoresh et al.*, 2008; *Dutkiewicz et al.*, 2009], but frequently, a single numerical phytoplankton species tends to outcompete most or all of the others [*Gregg et al.*, 2003; *Follows et al.*, 2007; *Dutkiewicz et al.*, 2009; *Sinha et al.*, 2010; *Barton et al.*, 2010]. This situation matches the well-known paradox of the plankton as formulated by *Hutchinson* [1961, p. 137]:

[5] "The problem that is presented by the phytoplankton is essentially how it is possible for a number of species to coexist in a relatively isotropic or unstructured environment all competing for the same sorts of materials. … According to the principle of competitive exclusion [*Hardin*, 1960] … we should expect that one species alone would outcompete all the others so that in a final equilibrium situation the assemblage would reduce to a population of a single species."

[6] Proposed solutions to the paradox, i.e. explanations for the observed phytoplankton diversity include environmental spatial and/or temporal heterogeneity, internally generated non-equilibrium dynamics as well as biological factors promoting diversity [*Roy and Chattopadhyay*, 2007]. Among the latter are different life-history patterns, differential resource

[1]GEOMAR, Helmholtz Centre for Ocean Research Kiel, Kiel, Germany.

Corresponding Author: L. Göthlich, GEOMAR, Helmholtz Centre for Ocean Research Kiel, Düsternbrooker Weg 20, D-24105 Kiel, Germany. (lgoethlich@geomar.de)

0886-6236/12/2011GB004042

Table 1. Parameters and Variables

Symbol	Definition	Unit
P_i	abundance of species i	$\mu mol\ C/l$ (chemostat model) $\mu mol\ P/l$ (global model)
R_j	concentration of resource j	$\mu mol/l$
μ_i	growth rate of species i	$1/d$
$C_{j,i}$	stoichiometric coefficient of resource j for species i	$mol/mol\ C$ (chemostat model) $mol/mol\ P$ (global model)
$K_{j,i}$	half-saturation constant of species i for uptake of resource j	$\mu mol/l$
r_i	maximum growth rate of species i	$1/d$
S_j	concentration of supply of resource j	$\mu mol/l$
D	dilution rate	$1/d$
k	number of resources	-
n	number of species	-

use and keystone predation [*Armstrong and McGehee*, 1980]. The present study focusses exclusively on differential resource use as presented by *Tilman* [1980] as a means of maintaining phytoplankton coexistence in biogeochemical models.

1.1. Theoretical Background

[7] The reason for the extinctions in recent phytoplankton models [*Bruggeman and Kooijman*, 2007; *Follows et al.*, 2007; *Shoresh et al.*, 2008; *Dutkiewicz et al.*, 2009] can be deduced using the R^* concept [*Dutkiewicz et al.*, 2009], which is part of Tilman's resource competition theory [*Tilman*, 1980]: In steady state, a monoculture of any species reduces the concentration of its limiting resource to the lowest concentration allowing for its survival (R^*), hence growth rate equals losses. In a multi-species assemblage, the species requiring the lowest resource concentration will set the equilibrium resource concentration to its resource requirement R^*, which is too low for any other species to survive. Yet in practice, there is no steady state and species must avoid exclusion only for the timescale of the system under consideration, which is usually several orders of magnitude longer than the lifetime of a phytoplankton cell. Species with very similar R^*s may coexist for long enough to survive in the ocean [*Dutkiewicz et al.*, 2009].

[8] For coexistence of several species in a steady-state system with two or more resources, each species must be limited by a different resource, for which is has a higher requirement than all of its competitors [*Petersen*, 1975; *Tilman*, 1980]. For n resources, this implies that at most n species can coexist. Yet in many models with multiple potentially limiting resources, the number of surviving species rarely reaches the number of limiting resources [*Follows et al.*, 2007; *Shoresh et al.*, 2008; *Dutkiewicz et al.*, 2009].

1.2. Scope of This Study

[9] To explain these earlier findings and to explore the potential of a simple and plausible model alteration in enhancing coexistence, we simulated phytoplankton communities in a simple chemostat [*Petersen*, 1975; *Huisman and Weissing*, 1999; *Shoresh et al.*, 2008] and in a global ocean model with a self-assembling phytoplankton community [*Follows et al.*, 2007; *Dutkiewicz et al.*, 2009]. In both models, each resource and phytoplankton species are modeled individually. Each species i is characterized by its half-saturation constants $K_{j,i}$ for the uptake of each nutrient j (for details see section 2.1), the stoichiometric ratio (i.e. the relative resource content) $C_{j,i}$ of each resource j with respect to carbon (chemostat model) or phosphorus (global model), and its maximum growth rate r_i. The impact of these parameters on coexistence are evaluated by numerical simulations of randomly assembled plankton communities. Particular attention is paid to the effects of varying the species' stoichiometric coefficients $C_{j,i}$, since in global plankton models those are commonly parameterized according to the Redfield Ratio [*Redfield*, 1934; *Gregg et al.*, 2003; *Dutkiewicz et al.*, 2009], so that all species have the same stoichiometry ($C_{j,i} = C_j$ for every species i). We compared modeled diversity in runs with identical stoichiometry (molar N:C = 0.15, P:C = 9.4×10^{-3}, Si:C = 0.15, Fe:C = 1.175×10^{-5} [*Redfield*, 1934; *Follows et al.*, 2007], Si only in chemostat model) to modeled diversity in simulations with stoichiometry drawn randomly from a $\pm$ 25% range around those values.

2. Model Description

2.1. Chemostat Model

[10] The standard model of resource competition in a chemostat [*Petersen*, 1975; *Tilman*, 1980] uses a Monod nutrient uptake function for the phytoplankton. The Monod equation originally describes growth as a saturating function of a single external resource concentration: Growth of species i is assumed proportional to $r_i R_j/(K_{ji} + R_j)$ for resources R_j and half-saturation constants $K_{j,i}$ and a maximum possible growth rate r_i. In this formulation, $K_{j,i}$ is the external resource concentration R_j at which half of the maximum growth rate r_i is achieved, i.e. the half-saturation constant. Since in the present study, several external resources are modeled, of which only one determines the growth rate at a given point in time, the Monod equation is used to determine the potential uptake for each resource separately, while only the most limiting resource determines a species' actual growth rate (Liebig's law of the minimum).

[11] Half-saturation constants for each resource were drawn randomly from the ranges suggested by *Follows et al.* [2007]. The stoichiometry of the individual species is fixed, and all species take up all resources. Thus, every species influences every resource and vice versa. Maximum growth rates were identical for all phytoplankton species in all experiments as was mortality, solely determined by the dilution rate. The model equations are as follows (for definitions of variables and parameters see Table 1, for parameter values and ranges see Table 2):

$$\frac{dP_i}{dt} = P_i(\mu_i(R_1, \ldots, R_k) - D) \quad i = 1, \ldots, n \tag{1}$$

$$\frac{dR_j}{dt} = D(S_j - R_j) - \Sigma_{i=1}^{n} C_{ji}\mu_i(R_i, \ldots, R_k)P_i \quad j = 1, \ldots, k \tag{2}$$

$$\mu_i(R_1, \ldots, R_k) = \min\left(\frac{r_i R_1}{K_{1i} + R_1}, \ldots, \frac{r_i R_k}{K_{ki} + R_k}\right) \tag{3}$$

Table 2. Parameter Values in Chemostat Model

Parameter	Definition	Min	Max	Unit
K_{NO_3}	half-saturation constant NO_3	0.24	0.56	$\mu mol/l$
K_{PO_4}	half-saturation constant PO_4	0.0135	0.035	$\mu mol/l$
K_{SiO_2}	half-saturation constant SiO_2	0.24	0.56	$\mu mol/l$
K_{Fe}	half-saturation constant Fe	1.7×10^{-5}	4.4×10^{-5}	$\mu mol/l$
C_N	stoichiometric coefficient N (cellular N:C)	0.135	0.165	$molN/mol\ C$
C_P	stoichiometric coefficient P (cellular P:C)	8.46×10^{-3}	10.34×10^{-3}	$molP/mol\ C$
C_{Si}	stoichiometric coefficient Si (cellular Si:C)	0.135	0.165	$molSi/mol\ C$
C_{Fe}	stoichiometric coefficient Fe (cellular Fe:C)	1.058×10^{-5}	1.293×10^{-5}	$molFe/mol\ C$
C_N^*	Redfield N:C	0.15	–	$molN/mol\ C$
C_P^*	Redfield P:C	9.4×10^{-3}	–	$molP/mol\ C$
C_{Si}^*	Redfield Si:C	0.15	–	$molSi/mol\ C$
C_{Fe}^*	Redfield Fe:C	1.175×10^{-5}	–	$molFe/mol\ C$
r_i	max. growth rate	2.0	–	$1/d$
D	dilution rate	0.25	–	$1/d$
S_{NO_3}	NO_3 supply	16	–	$\mu mol/l$
S_{PO_4}	PO_4 supply	1	–	$\mu mol/l$
S_{SiO_2}	SiO_2 supply	16	–	$\mu mol/l$
S_{Fe}	Fe supply	0.0125	–	$\mu mol/l$

[12] The chemostat model was initialized with 8 species and 4 resources, namely nitrate, phosphate, silicate, and iron, and run for 20 years. Concentrations of nutrient supply were 16 $\mu molNO_3/l$, 16 $\mu molSiO_2/l$, 1 $\mu molPO_4/l$ and 0.0125 $\mu molFe/l$. Each different model configuration was run 50 times with different parameter sets owing to the random assignments involved. Phytoplankton was initialized with a concentration of $1\mu molC/l$. Any species reaching a concentration of less than $10^{-8}\mu molC/l$ was considered extinct and was removed from the system. This ensured numerical stability and prevented the unrealistic re-appearance of a practically extinct species in unstable systems. For the number of surviving species, only species with a concentration of $\geq 10^{-3}\mu molC/l$ were taken into account.

2.2. Global Model

[13] The global marine ecosystem model is a modified version of the self-assembling marine ecosystem model by *Follows et al.* [2007] comprising 78 phytoplankton and 2 zooplankton types. It explicitly resolves ocean circulation and mixing on a $1 \times 1^\circ$ grid with 23 depth levels. This model has previously been examined with regard to resource competition theory [*Dutkiewicz et al.*, 2009; *Barton et al.*, 2010] and this approach is extended in this study by including the effect of species-dependent phytoplankton stoichiometry.

[14] The global model explicitly simulates the nutrients phosphorus, nitrate, nitrite, ammonia, silicate and iron, with phosphorus being used as the currency nutrient. It uses one prognostic equation for each of the 78 phytoplankton types and the 2 zooplankton types. Phytoplankton growth depends on light, nutrients, and temperature, while phytoplankton mortality is due to grazing, sinking, and a non-specific linear mortality.

[15] The original *Follows et al.* [2007] model randomly assigns parameter values (from predefined ranges) for temperature, light, and nutrient dependence to 78 different phytoplankton types. For this study, the version by *Dutkiewicz et al.* [2009] is used, but all randomness with regard to light and temperature dependence is removed. Of the originally 4 different functional phytoplankton types only the small functional type is used, albeit with a slightly increased maximum growth rate and the ability to use all forms of nitrogen (nitrate, nitrite and ammonia). Since all 78 phytoplankton types are of the same type and their nutrient uptake parameters are drawn from the same range, all competitive exclusion is due to differences in nutrient uptake capacity and not due to other interspecific variations. For the detailed parameter values see Table 3. Diatoms are not simulated in this study, hence silicate parameters are omitted.

[16] Since for equilibrium coexistence it is crucial that each species is a poor competitor for at least one of the resources, a simple trade-off between different Ks for each species was introduced: K_{PO_4} is drawn randomly from the range defined in Table 3:

$$K_{PO_4} = K_{PO_4}^{\min} + rand_1 * (K_{PO_4}^{\max} - K_{PO_4}^{\min}) \quad (4)$$

[17] where *rand* is a random number distributed uniformly between 0 and 1. The difference between K_{PO_4} and $K_{PO_4}^{\min}$ is then used to generate K_{NO_3} in such a way that a species with a low K_{PO_4} has a high K_{NO_3} and vice versa:

$$K_{NO_3} = K_{NO_3}^{\max} - \frac{K_{PO_4} - K_{PO_4}^{\min}}{K_{PO_4}^{\max} - K_{PO_4}^{\min}} * (K_{NO_3}^{\max} - K_{NO_3}^{\min}) \quad (5)$$

A new random number between 0 and 1 is used to allow for 10% variability:

$$K_{NO_3} = K_{NO_3} \pm 0.1 * rand_2 * K_{NO_3} \quad (6)$$

K_{Fe} is traded off against K_{NO_3} in the same way:

$$K_{Fe} = K_{Fe}^{\max} - \frac{K_{NO_3} - K_{NO_3}^{\min}}{K_{NO_3}^{\max} - K_{NO_3}^{\min}} * (K_{Fe}^{\max} - K_{Fe}^{\min}) \quad (7)$$

$$K_{Fe} = K_{Fe} \pm 0.1 * rand_3 * K_{Fe} \quad (8)$$

[18] This leads to K_{Fe} and K_{PO_4} being positively correlated, but iron and phosphate limitation do not spatially

Table 3. Parameter Values in Global Model

Parameter	Definition	Min	Max	Unit
K_{PO_4}	half-saturation constant PO_4	0.015	0.035	μM
K_{NO_3}	half-saturation constant NO_3	0.18	0.70	μM
K_{NO_2}	half-saturation constant NO_2	0.18	0.70	μM
K_{NH_4}	half-saturation constant NH_4	0.09	0.35	μM
K_{Fe}	half-saturation constant Fe	1.125×10^{-5}	4.375×10^{-5}	μM
$C_{N:P}$	stoichiometric coefficient N (cellular N:P)	12	20	*mol N/mol P*
$C_{C:P}$	stoichiometric coefficient C (cellular C:P)	90	150	*mol C/mol P*
$C_{Fe:P}$	stoichiometric coefficient Fe (cellular Fe:P)	0.75×10^{-3}	1.25×10^{-3}	*mol Fe/mol P*
$C^*_{N:P}$	Redfield N:P	16	–	*mol N/mol C*
$C^*_{C:P}$	Redfield C:P	120	–	*mol C/mol P*
$C^*_{Fe:P}$	Redfield Fe:P	1.0×10^{-3}	–	*mol Fe/mol P*
r_i	max. growth rate	2.2	–	$1/d$
m_i	mortality	0.1	–	$1/d$

coincide in this model (see Figure 1). So this lack of a trade-off was accepted for simplicity.

[19] K_{NO_2} and K_{NH_4} are assigned relative to K_{NO_3}:

$$K_{NO_3} = K_{NO_2} = 2{*}K_{NH_4} \tag{9}$$

[20] Stoichiometry in the runs with species-specific stoichiometry is proportional to the ratios of the Ks, i.e. $C_{x:P} = K_x/K_{PO_4}$. The ratio of P to carbon is assigned so that a species with a high K_{PO_4} has a high $C_{P:C}$, i.e. a species likely to be limited by PO_4 also consumes a lot of PO_4. This facilitates the occurrence of stable equilibrium conditions (for details see section 3.2). In the runs with Redfield stoichiometry, the Ks are the same as in those with species-specific stoichiometry, whereas the Cs are the same as in the original model.

3. Chemostat Model Results

3.1. Redfield Stoichiometry

[21] In a first set of chemostat experiments all species are assigned the same stoichiometry. The first configuration, $C_{\mathrm{Redf}}K_{\mathrm{rand}}$, uses Redfield stoichiometry and randomly chosen half-saturation constants $K_{j,i}$ for the different resources j and species i. Altogether, 50 simulations are performed, each starting with 8 random species and 4 resources, hence the equilibrium number of species cannot exceed 4. After 20 years, the number of surviving phytoplankton species rarely exceeds one and never exceeds two (Figure 2a). 20 years is a typical advective timescale for an oligotrophic gyre, an oceanic system to which a chemostat model is closer than to more dynamic systems with shorter timescales.

[22] In the second set of experiments, it was considered that careful ranking of the different equilibrium resource concentrations $R^*_{i,j}$ for each resource j can enhance coexistence [*Huisman and Weissing*, 2001]: Each species has to be the worst competitor for one resource, i.e. for every resource j one species i has the maximum R^*_j. This ensures that each species is limited by a different resource, namely the one for which it has the highest R^*. Since in this chemostat model, maximum growth rates r_i and mortality (i.e. dilution) rates D are identical for all species, differences in R^* are solely determined by the half-saturation constants $K_{j,i}$ ($R^*_{i,j} = K_{j,i}D/(r - D)$). This configuration is referred to as $C_{\mathrm{Redf}}K_{\mathrm{rank}}$, and uses half-saturation constants $K_{j,i}$ so that two species are limited by resource one, two species by resource two etc., of which at most one species is expected to survive. However,

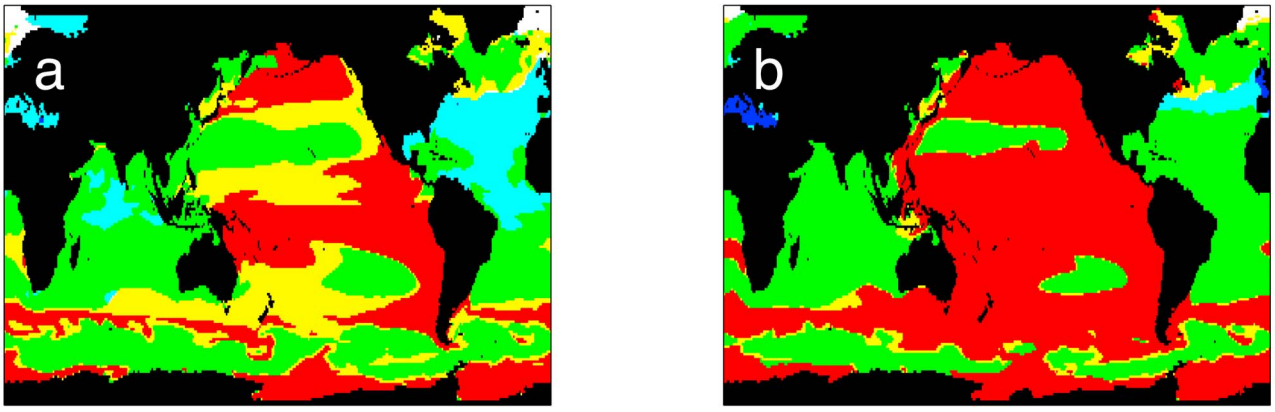

Figure 1. Limiting nutrient of all species in year 10 of the integration, upper 5 m. (a) Species-specific stoichiometry. (b) Redfield stoichiometry. Green: N limitation only; red: Fe limitation only; blue: P limitation only; mixtures indicate limitation of different algae by different nutrients, regardless of the respective number of species each; cyan: N and P limitation; yellow: N and Fe limitation; magenta: P and Fe limitation.

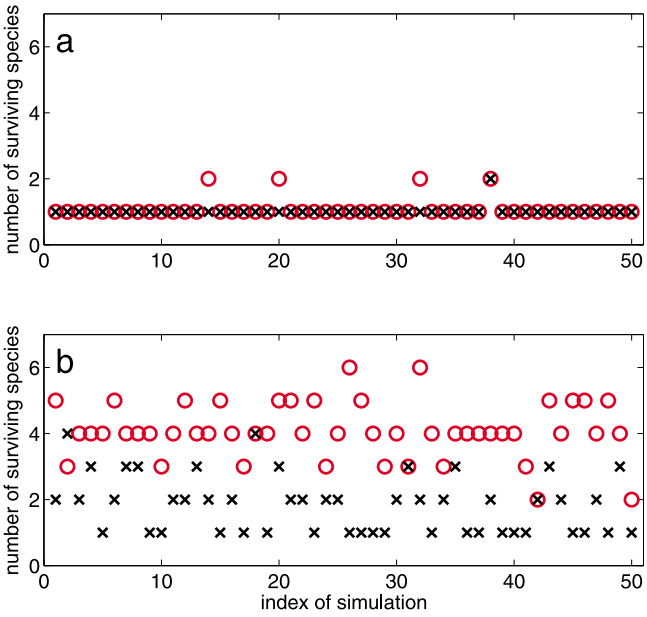

Figure 2. Number of surviving species at the end of 50 simulations over 20 years each. (a) Configurations $C_{\mathrm{Redf}}K_{\mathrm{rand}}$ (black crosses) and $C_{\mathrm{Redf}}K_{\mathrm{rank}}$ (red circles) and (b) configurations $C_{\mathrm{eq}}K_{\mathrm{rand}}$ (black crosses) and $C_{\mathrm{eq}}K_{\mathrm{rank}}$ (red circles). Model configurations are described in Table 4.

also in configuration $C_{\mathrm{Redf}}K_{\mathrm{rank}}$ the number of coexisting species rarely exceeds one and never exceeds two (Figure 2a).

[23] The chemostat simulations using the same (Redfield) stoichiometry for all species with random half-saturation constants for nutrient uptake do not allow for steady-state phytoplankton coexistence, in agreement with earlier theoretical studies [*Tilman*, 1980; *Huisman and Weissing*, 2001]. Since in all simulations the maximum growth rate r_i is the same for all species, one might argue whether more species might coexist for species-specific values of r_i. Following *Shoresh et al.* [2008] it can, however, be shown that stable coexistence is impossible when all species obey the same stoichiometry, irrespective of their maximum growth rates (see Appendix A).

3.2. Interspecies Stoichiometric Variations

[24] Another series of simulations was run using different stoichiometries among the different species with $C_{j,i}$ assigned to match the conditions for coexistence [*Huisman and Weissing*, 2001]: Each species consumes most of the resource by which it is limited; $K_{j,i}$ are assigned randomly in configuration $C_{\mathrm{eq}}K_{\mathrm{rand}}$, and for each resource j the species i with highest $K_{j,i}$ gets the highest value of $C_{j,i}$ among all species. In configuration $C_{\mathrm{eq}}K_{\mathrm{rank}}$, the $K_{j,i}$ and $C_{j,i}$ are assigned according to equilibrium conditions so that each species is limited by the resource of which it consumes most. For details on the parameterization see Tables 2 and 4.

[25] For the same random choices of $K_{j,i}$ as in the two respective Redfield experiments, the chance for coexistence increases significantly in the simulations with species-specific stoichiometries chosen such that each species consumes most of the resource for which it has the highest requirement (Figure 2): Among all simulation experiments performed, the by far highest number of coexisting phytoplankton species (4.08 ± 0.85) is reached in experiment $C_{\mathrm{eq}}K_{\mathrm{rank}}$, for which the $K_{j,i}$ and the $C_{j,i}$ are chosen so that both the conditions for the existence of a 4-species-equilibrium ($K_{j,i}$) and the conditions for said equilibrium to be stable ($C_{j,i}$) are met. Whenever species numbers exceed 4 (number of resources), competitive exclusion is not yet complete. Incomplete exclusion also occurred in the other configurations, which reach average numbers of coexisting species of 1.84 ± 0.87 in experiment $C_{\mathrm{eq}}K_{\mathrm{rand}}$, 1.08 ± 0.27 in $C_{\mathrm{Redf}}K_{\mathrm{rank}}$ and 1.02 ± 0.14 in $C_{\mathrm{Redf}}K_{\mathrm{rand}}$.

4. Global Model Results

[26] The results of the global model mirror those of the chemostat model: phytoplankton diversity is, on average, higher in the run with species-specific stoichiometry compared to the run employing Redfield stoichiometry for all species (see Figure 3). Diversity is distinctly increased in the North Atlantic, the North Pacific and the Indian Ocean,

Table 4. Parameter Assignment for Chemostat Simulations

Configuration	$K_{j,i}$	$C_{j,i}$	Details for $K_{j,i}$	Details for $C_{j,i}$
$C_{\mathrm{Redf}}K_{\mathrm{rand}}$	random	Redfield	randomly from ranges defined in Table 2	$C_{j,i} = C_j^*$, see Table 2
$C_{\mathrm{Redf}}K_{\mathrm{rank}}$	ranked	Redfield	as in experiment $C_{\mathrm{Redf}}K_{\mathrm{rand}}$, with each K_{ii} increased (by a random amount of max. 10%) above the maximum of the predefined range, in order to obtain a rank order so that species 1 is the worst competitor for resource 1, species 2 is the worst competitor for resource 2, etc.	$C_{j,i} = C_j^*$, see Table 2
$C_{\mathrm{eq}}K_{\mathrm{rand}}$	random	equilibrium[a]	randomly from ranges defined in Table 2	$C_{j,i}$ drawn randomly from the stoichiometric ranges of Table 2. The $C_{j,i}$ for the species with highest $K_{j,i}$ for each resource j gets assigned a value 10% larger than the upper limit of this range.
$C_{\mathrm{eq}}K_{\mathrm{rank}}$	ranked	equilibrium[a]	as in experiment $C_{\mathrm{Redf}}K_{\mathrm{rand}}$, with each K_{ii} increased (by a random amount of max. 10%) above the maximum of the predefined range, in order to obtain a rank order so that species 1 is the worst competitor for resource 1, species 2 is the worst competitor for resource 2, etc.	$C_{j,i}$ drawn randomly from the stoichiometric ranges of Table 2. The $C_{j,i}$ for the species with highest $K_{j,i}$ for each resource j gets assigned a value 10% larger than the upper limit of this range.

[a]Conditions for stability of equilibrium according to *Huisman and Weissing* [2001].

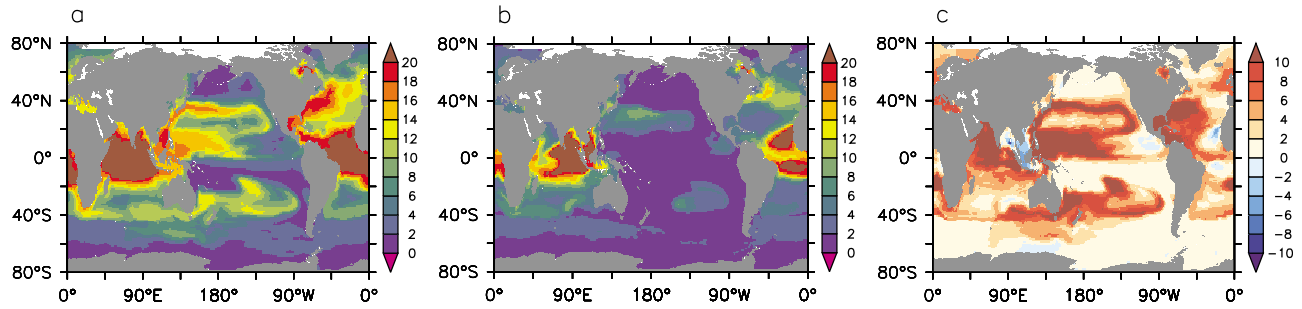

Figure 3. Number of surviving species in the upper 55 m of the global model after 10 years: (a) 25% variability in stoichiometry, (b) Redfield stoichiometry, and (c) difference.

whereas in the South Pacific and the Southern Ocean the difference is less pronounced. The cause and implication of these results are discussed in section 5.2.

5. Discussion

5.1. Chemostat Model

[27] In the chemostat experiments, only species-specific stoichiometric ratios chosen in such a way that each species consumes most of the resource for which it has the highest requirement among the coexisting species (highest half-saturation constant $K_{j,i}$ for a given resource j) allows for coexistence with each species being limited by a different resource. This conclusion is consistent with those of earlier studies [*Petersen*, 1975; *Tilman*, 1980]. This stability criterion was extended analytically to a hypothetical three-resource system by *Huisman and Weissing* [2001]. In the present study, it has been extended further to a four-resource system representing nitrate, phosphate, silicate, and iron, generally thought to be the most limiting nutrients in the global ocean [*Falkowski et al.*, 1998]. Parameters were chosen to resemble those of actual oceanic phytoplankton, thereby linking resource competition theory and global biogeochemical modeling applications.

5.2. Global Model

[28] Both conditions for stable coexistence can also be attained in the global model simulations. Since in the original configuration [*Dutkiewicz et al.*, 2009] the ratios of the different $K_{j,i}$ were identical for all species, all species in one place were almost always limited by the same resource. In the current study, the ratios of the different $K_{j,i}$ were allowed to vary between species, hence different species can be limited by different resources in one place.

[29] In the Atlantic and Pacific, and to a lesser extent in the Indian and Southern Ocean, large areas show limitation by two nutrients in the species-specific-stoichiometry run (see Figure 1a, $75.36*10^6$ km^2 N and P limitation, $38.56*10^6$ km^2 N and Fe limitation). With Redfield stoichiometry applied, limitation of different algae by different nutrients is restricted to considerably smaller areas (see Figure 1b, $14.49*10^6$ km^2 N and P limitation, $5.55*10^6$ km^2 N and Fe limitation). Since stoichiometry determines nutrient uptake ratios in this model, this shows that nutrient uptake ratios can have considerable influence on nutrient concentrations in addition to their impact on diversity.

5.3. Niche Theory

[30] Nutrient uptake ratios ($C_{j,i}$) are part of a species' ecological "impact niche", which is the impact an organism has on its environment by consuming resources [*Leibold*, 1995], representing one of the two concepts of an ecological niche. The complementary niche concept is the "requirement niche", encompassing the impact of the environment on an organism. While the requirement niche, represented by $K_{j,i}$, is often paid attention in biogeochemical models including the one used in this study [*Dutkiewicz et al.*, 2009; *Barton et al.*, 2010], the impact niche is mostly ignored through the widespread implementation of constant (generally Redfield) stoichiometry, which essentially creates one identical impact niche for all species. Yet, in reality species do have different impacts on their environment and thereby influence the requirement niches of other species as well as their own. This connection is mirrored in the global model results presented in this study: Different nutrient uptake ratios (impact niches) lead to different species being limited by different resources (requirement niches). Identical nutrient uptake ratios impede that effect. In addition, the imposed positive correlation between the $C_{j,i}$ and the $K_{j,i}$ implies that through their impact niches, each species has a stronger influence on its own requirement niche than on that of other species. By taking up most of the nutrient it requires most, it limits its own growth more than it limits others, i.e. intraspecific competition is greater than interspecific competition, a mechanism that is known to promote diversity [*Chesson*, 2000; *Tilman*, 1980].

5.4. Parameter Choices

[31] This positive correlation between the $C_{j,i}$ and the $K_{j,i}$ (or R^*) imposed in the model is supported by data for some of the nutrients used in this study: Different algae show strong positive correlation between C_{Si} and R^*_{Si} [*Huisman and Weissing*, 2001] and there is also evidence for a positive correlation between the minimum nitrogen content $C_{N_{min}}$ and half-saturation constants K_{NO_3} and K_{NH_4} [*Litchman et al.*, 2007; *Sunda and Hardison*, 2010], respectively. Low C_{Fe} is found in small oceanic phytoplankton species with a high surface-to-volume ratio enabling fast nutrient uptake (low K_{Fe}). Coastal phytoplankton have higher values for both parameters [*Sunda and Huntsman*, 1995].

[32] Besides the link between $C_{j,i}$s and $K_{j,i}$s, stable coexistence also assumes trade-offs between the $K_{j,i}$ for each species i. Data on R^* [*Huisman and Weissing*, 2001] show

trade-offs for phosphate vs. silicate and nitrate vs. silicate in diatoms. For other resources, similar trade-offs are not known, but are considered plausible as a result of physiological limits on nutrient acquisition [*Litchman and Klausmeier*, 2008].

[33] A next step towards simulating resource use and uptake by phytoplankton more realistically would be to explicitly simulate the changes in stoichiometry in response to ambient concentrations and phytoplankton growth. Available models with different levels of sophistication include Droop's cell quota model [*Droop*, 1973] as well as Pahlow's optimal growth model using explicit dynamics for various phytoplankton properties [*Pahlow*, 2005; *Pahlow and Oschlies*, 2009]. However, such models are computationally more expensive and differ in more than one aspect with respect to the standard constant-stoichiometry model version. The current study attempts to apply a minimum variation to the standard model and thereby conclusively attribute all changes in model dynamics to the only change of allowing small variations in the phytoplankton's stoichiometry.

6. Conclusion

[34] While it is unclear whether the proposed mechanism of stoichiometrically generated impact niches is crucial in maintaining phytoplankton diversity in the ocean, there is sufficient data showing that the Redfield Ratio is only valid when averaging over many species. Individual species' stoichiometric coefficients differ from one another, and those of one species differ in time and space [*Geider and La Roche*, 2002; *Anderson and Pondaven*, 2003; *Klausmeier et al.*, 2004]. Combining the findings of this study with evidence from data supports the need for going beyond the Redfield Ratio as a common stoichiometry in models with multiple phytoplankton compartments. Instead, species' resource contents should vary across species, and, if coexistence in models is to be sustained to allow for conclusions about environmentally induced changes in community compositions, the conditions for stable coexistence should be considered.

Appendix A: Analysis of Redfield Case

[35] In this appendix, the stability of a multispecies equilibrium with the same stoichiometry assigned to all species is analyzed in detail. Assuming the $R^*_{i,j}$, dependent on half-saturation constants, dilution and maximum uptake rate, are chosen in such a way that each species i is limited by a different resource j (species 1 by resource 1, species 2 by resource 2 and so on), [*Shoresh et al.*, 2008] derived the general conditions for a given equilibrium to be stable, based on the steady-state solution of equations 1 and 2.

$$\frac{dP_i}{dt} = P_i\left(\frac{r_i R_i}{K_{ii}+R_i} - D\right) = 0 \longleftrightarrow \mathbf{R}^* = \frac{D\mathbf{K}}{r-D} \tag{A1}$$

$$\frac{dR_j}{dt} = D(S_j - R_j) - \sum_{i=1}^{n} C_{ji}P_i\frac{r_i R_i}{K_{ii}+R_i} = 0 \longleftrightarrow$$
$$\mathbf{P}^* = \mathbf{C}^{-1}\left(\mathbf{S} - \frac{D\mathbf{K}}{r-D}\right) \tag{A2}$$

and using the following vector notation:

$$\mathbf{P} = \begin{pmatrix} P_1 \\ \vdots \\ P_n \end{pmatrix},\ \mathbf{K} = \begin{pmatrix} K_{11} \\ \vdots \\ K_{nn} \end{pmatrix},\ \mathbf{S} = \begin{pmatrix} S_1 \\ \vdots \\ S_n \\ \hline S_{n+1} \\ \vdots \\ S_k \end{pmatrix},\ \mathbf{R} = \begin{pmatrix} R_1 \\ \vdots \\ R_n \\ \hline R_{n+1} \\ \vdots \\ R_k \end{pmatrix} = \begin{pmatrix} \bar{\mathbf{R}} \\ \hline \tilde{\mathbf{R}} \end{pmatrix},$$
$$\mathbf{C} = \left(\begin{array}{ccc} C_{11} & \ldots\ldots & C_{1n} \\ \vdots & \ddots & \vdots \\ C_{n1} & \ldots\ldots & C_{nn} \\ \hline C_{n+11} & \ldots\ldots & C_{n+1n} \\ \vdots & \ddots & \vdots \\ C_{k1} & \ldots\ldots & C_{kn} \end{array}\right) = \begin{pmatrix} \bar{\mathbf{C}} \\ \hline \tilde{\mathbf{C}} \end{pmatrix}.$$

[36] Where $i = 1, \ldots, n$, with n being the number of species, $j = 1, \ldots, k$, with k being the number of resources and $n \le k$, $C_{j,i}$ the stoichiometric coefficient of species i for resource j, $K_{i,i}$ the half-saturation constant of species i for its limiting resource, P^*_i the equilibrium concentration of species i, r_i the maximum growth rate of species i, D the dilution rate (=mortality).

[37] Stability of the equilibrium solution (marked by an asterisk) can be investigated by adding a small perturbation δ and keeping only terms that are linear in δ: $\mathbf{P} = \mathbf{P}^* + \delta\mathbf{P}$, $\bar{\mathbf{R}} = \bar{\mathbf{R}}^* + \delta\bar{\mathbf{R}}$ and $\tilde{\mathbf{R}} = \bar{\mathbf{R}}^* + \delta\tilde{\mathbf{R}}$.

[38] This leads to

$$\frac{d}{dt}\begin{pmatrix} \delta\mathbf{P} \\ \delta\bar{\mathbf{R}} \\ \delta\tilde{\mathbf{R}} \end{pmatrix} = \mathbf{J}\begin{pmatrix} \delta\mathbf{P} \\ \delta\bar{\mathbf{R}} \\ \delta\tilde{\mathbf{R}} \end{pmatrix} \tag{A3}$$

with the Jacobian

$$\mathbf{J} = \begin{pmatrix} 0 & \mathbf{A} & 0 \\ -D\bar{\mathbf{C}} & -D\bar{\mathbf{I}} - \bar{\mathbf{F}} & 0 \\ -D\tilde{\mathbf{C}} & \tilde{\mathbf{F}} & -D\tilde{\mathbf{I}} \end{pmatrix},$$

with

$$\mathbf{A}_{n\times n} = \{A_{ij}\},\ A_{ij} = \frac{P^*_i(r_i - D)^2}{r_i K_{ii}}\delta_{ij},\ i,j = 1, \ldots, n \tag{A4}$$

$$\bar{\mathbf{F}}_{n\times n} = \{\bar{F}_{ji}\},\ \bar{F}_{ji} = C_{ji}A_{ii},\ i,j = 1, \ldots, n \tag{A5}$$

$$\tilde{\mathbf{F}}_{(k-n)\times n} = \{\tilde{F}_{ji}\},\ \tilde{F}_{ji} = C_{ji}A_{ii},\ j = n+1, \ldots, k, i = 1, \ldots, n \tag{A6}$$

and $\bar{\mathbf{I}}_{n\times n}$ and $\tilde{\mathbf{I}}_{(k-n)\times(k-n)}$ being identity matrices.

[39] For the equilibrium to be stable, all eigenvalues of $\mathbf{J}$ need to be negative. *Shoresh et al.* [2008] then derive that this is the case if and only if all the eigenvalues of the matrix $\bar{\mathbf{F}}$ with

$$\bar{F}_{ji} = \frac{(r_i - D)^2 C_{ji}P^*_i}{r_i K^*_{ii}} \tag{A7}$$

are positive. Setting C_{ji} in such a way that all species are assigned the same stoichiometry (i.e. $C_{j1} = C_{j2}, \ldots, = C_{jn}$ etc.) leads to

$$\bar{F}_{ji} = \frac{(r_i - D)^2 C_j P^*_i}{r_i K^*_{ii}}. \tag{A8}$$

[40] Since r_i, K_{ii}^* and P_i^* differ only between species, while C_j differs only between resources, $\bar{F}_{ji}$ can be split into the resource-dependent part C_j and a species-dependent term B_i, so that

$$B_i = \frac{(r_i - D)^2 P_i^*}{r_i K_{ii}^*}. \tag{A9}$$

[41] Accordingly simplified, **F** becomes

$$\bar{F}_{ji} = \begin{vmatrix} B_1C_1 & B_2C_1 & \dots & B_nC_1 \\ B_1C_2 & B_2C_2 & \dots & B_nC_2 \\ \vdots & \vdots & \ddots & \vdots \\ B_1C_n & B_2C_n & \dots & B_nC_n \end{vmatrix}.$$

[42] The rows of **F** differ only by a factor (C_j) and are therefore linearly dependent, hence all eigenvalues of **F** except one are zero. Accordingly, the equilibrium point is not stable and all but one species will go extinct. Note that the instability of an equilibrium with coexisting species holds irrespective of whether or not the maximum growth rate r_i varies between species.

[43] **Acknowledgments.** The authors thank S. Dutkiewicz (MIT) for providing the global model code and F. Prowe (IFM-GEOMAR) for running the global model simulations. L.G. acknowledges funding by WGL-PAKT, project TiPI and the Deutsche Forschungsgemeinschaft (DFG) via SFB 754.

References

Anderson, T., and P. Pondaven (2003), Non-Redfield carbon and nitrogen cycling in the Sargasso Sea: Pelagic imbalances and export flux, *Deep Sea Res., Part II*, *50*(5), 573–591, doi:10.1016/S0967-0637(03)00034-7.

Armstrong, R., and R. McGehee (1980), Competitive exclusion, *Am. Nat.*, *115*, 151–170.

Barton, A., S. Dutkiewicz, G. Flierl, J. Bragg, and M. Follows (2010), Patterns of diversity in marine phytoplankton, *Science*, *327*(5972), 1509–1511, doi:10.1126/science.1184961.

Behrenfeld, M., et al. (2006), Climate-driven trends in contemporary ocean productivity, *Nature*, *444*(7120), 752–755, doi:10.1038/nature05317.

Boyce, D., M. Lewis, and B. Worm (2010), Global phytoplankton decline over the past century, *Nature*, *466*(7306), 591–596, doi:10.1038/nature09268.

Bruggeman, J., and S. Kooijman (2007), A biodiversity-inspired approach to aquatic ecosystem modeling, *Limnol. Oceanogr.*, *52*(4), 1533–1544.

Chesson, P. (2000), Mechanisms of maintenance of species diversity, *Annu. Rev. Ecol. Syst.*, *31*, 343–366.

Droop, M. (1973), Some thoughts on nutrient limitation in algae, *J. Phycol.*, *9*(1973), 264–272.

Dutkiewicz, S., M. Follows, and J. Bragg (2009), Modeling the coupling of ocean ecology and biogeochemistry, *Global Biogeochem. Cycles*, *23*, GB4017, doi:10.1029/2008GB003405.

Falkowski, P., R. Barber, and V. Smetacek (1998), Biogeochemical controls and feedbacks on ocean primary production, *Science*, *281*(5374), 200–206.

Follows, M., S. Dutkiewicz, S. Grant, and S. Chisholm (2007), Emergent biogeography of microbial communities in a model ocean, *Science*, *315* (5820), 1843–1846, doi:10.1126/science.1138544.

Geider, R., and J. La Roche (2002), Redfield revisited: Variability in the N:P ratio of phytoplankton and its biochemical basis, *Eur. J. Phycol.*, *37*, 1–17, doi:10.1017/S0967026201003456.

Gregg, W., P. Ginoux, P. Schopf, and N. Casey (2003), Phytoplankton and iron: Validation of a global three-dimensional ocean biogeochemical model, *Deep Sea Res., Part II*, *50*(22–26), 3143–3169, doi:10.1016/j.dsr2.2003.07.013.

Gregg, W., N. Casey, and C. McClain (2005), Recent trends in global ocean chlorophyll, *Geophys. Res. Lett.*, *32*, L03606, doi:10.1029/2004GL021808.

Hardin, G. (1960), The competitive exclusion principle, *Science*, *131*(3409), 1292–1297.

Hays, G., A. Richardson, and C. Robinson (2005), Climate change and marine plankton, *Trends Ecol. Evol.*, *20*(6), 337–344, doi:10.1016/j.tree.2005.03.004.

Hoegh-Guldberg, O., and J. Bruno (2010), The impact of climate change on the world's marine ecosystems, *Science*, *328*(5985), 1523, doi:10.1126/science.1189930.

Huisman, J., and F. Weissing (1999), Biodiversity of plankton by species oscillations and chaos, *Nature*, *402*(6760), 407–410.

Huisman, J., and F. Weissing (2001), Biological conditions for oscillations and chaos generated by multispecies competition, *Ecology*, *82*(10), 2682–2695.

Hutchinson, G. (1961), The paradox of the plankton, *Am. Nat.*, *95*(882), 137–145.

Klausmeier, C., E. Litchman, T. Daufresne, and S. Levin (2004), Optimal nitrogen-to-phosphorus stoichiometry of phytoplankton, *Nature*, *429*(6988), 171–174, doi:10.1038/nature02454.

Leibold, M. (1995), The niche concept revisited: Mechanistic models and community context, *Ecology*, *76*(5), 1371–1382.

Litchman, E., and C. Klausmeier (2008), Trait-based community ecology of phytoplankton, *Annu. Rev. Ecol. Syst.*, *39*(1), 615–639, doi:10.1146/annurev.ecolsys.39.110707.173549.

Litchman, E., C. Klausmeier, O. Schofield, and P. Falkowski (2007), The role of functional traits and trade-offs in structuring phytoplankton communities: Scaling from cellular to ecosystem level, *Ecol. Lett.*, *10*(12), 1170–1181, doi:10.1111/j.1461-0248.2007.01117.x.

McCann, K. (2000), The diversity–stability debate, *Nature*, *405*(6783), 228–233.

Pahlow, M. (2005), Linking chlorophyll-nutrient dynamics to the Redfield N:C ratio with a model of optimal phytoplankton growth, *Mar. Ecol. Prog. Ser.*, *287*, 33–43.

Pahlow, M., and A. Oschlies (2009), Chain model of phytoplankton P, N and light colimitation, *Mar. Ecol. Prog. Ser.*, *376*, 69–83, doi:10.3354/meps07748.

Petersen, R. (1975), The paradox of the plankton: An equilibrium hypothesis, *Am. Nat.*, *109*(965), 35–49.

Polovina, J., E. Howell, and M. Abecassis (2008), Ocean's least productive waters are expanding, *Geophys. Res. Lett.*, *35*, L03618, doi:10.1029/2007GL031745.

Redfield, A. (1934), On the proportions of organic derivatives in sea water and their relation to the composition of plankton, in *James Johnston Memorial Volume*, pp. 176–192, Univ. Press of Liverpool, Liverpool, U. K.

Richardson, A., and D. Schoeman (2004), Climate impact on plankton ecosystems in the northeast Atlantic, *Science*, *305*(5690), 1609–1612, doi:10.1126/science.11009581.

Roy, S., and J. Chattopadhyay (2007), Towards a resolution of the 'paradox of the plankton': A brief overview of the proposed mechanisms, *Ecol. Complexity*, *4*(1–2), 26–33, doi:10.1016/j.ecocom.2007.02.016.

Sarmiento, J., T. Hughes, R. Stouffer, and S. Manabe (1998), Simulated response of the ocean carbon cycle to anthropogenic climate warming, *Nature*, *393*(6682), 245–249.

Shoresh, N., M. Hegreness, and R. Kishony (2008), Evolution exacerbates the paradox of the plankton, *Proc. Natl. Acad. Sci. U. S. A.*, *105*(34), 12,365–12,369, doi:10.1073/pnas.0803032105.

Sinha, B., E. Buitenhuis, C. Quéré, and T. Anderson (2010), Comparison of the emergent behavior of a complex ecosystem model in two ocean general circulation models, *Prog. Oceanogr.*, *84*, 204–224, doi:10.1016/j.pocean.2009.10.003.

Sunda, W., and D. Hardison (2010), Evolutionary tradeoffs among nutrient acquisition, cell size, and grazing defense in marine phytoplankton promote ecosystem stability, *Mar. Ecol. Prog. Ser.*, *401*, 63–76, doi:10.3354/meps08390.

Sunda, W., and S. Huntsman (1995), Iron uptake and growth limitation in oceanic and coastal phytoplankton, *Mar. Chem.*, *50*(1–4), 189–206.

Tilman, D. (1980), Resources: A graphical-mechanistic approach to competition and predation, *Am. Nat.*, *116*(3), 362–393.